Effects of developmental age, brain region and time in culture on long-term proliferation and multipotency of neural stem cell populations

A. GRITTI, M. DAL MOLIN, C. FORONI, L. BONFANTI (2009) **Effects of developmental age, brain region and time in culture on long-term proliferation and multipotency of neural stem cell populations,** JOURNAL OF COMPARATIVE NEUROLOGY (ISSN:0021-9967), pp. 333- 349. Vol. 517.

DOI: 10.1002/cne.22153

Effects of developmental age, brain region and time in culture on long-term proliferation and multipotency of neural stem cell populations

A. GRITTI, M. DAL MOLIN, C. FORONI, L. BONFANTI

Abstract

Neural stem cells (NSCs) in the murine subventricular zone (SVZ) niche allow life-long neurogenesis. During the first postnatal month and throughout aging, the decrease of neuroblasts and the rise of astrocytes results in diminished neurogenesis and increased astrocyte:neuron ratio. Also, a different neurogenic activity characterizes the SVZ periventricular region (LV, lateral ventricle) as compared to its rostral extension (RE). In order to investigate whether and to what extent these physiological modifications may be ascribed to intrinsic changes of the endogenous NSC/progenitor features, we performed a functional analysis on NSCs isolated and cultured from LV and RE tissues at distinct postnatal stages that are marked by striking modifications to the SVZ niche in vivo. We evaluated the effect of age and brain region on long-term proliferation and multipotency, and characterized the cell type composition of NSC-derived progeny, comparing this make-up to that of region- and age-matched primary neural cultures. Furthermore, we analyzed the effect of prolonged in vitro expansion on NSC functional properties. We documented age- and region-dependent differences on the clonogenic efficiency and on the long-term proliferative capacity of NSCs. Also, we found age- and region-dependent quantitative changes in the cell composition of NSC progeny (decreased quantity of neurons and oligodendrocytes; increased amount of astroglial cells) and these differences were maintained in long-term cultured NSC populations. Overall, these data strengthen the hypothesis that age- and region-dependent differences in neurogenesis (observed in vivo) may be ascribed to the changes in the intrinsic developmental program of the NSC populations.

_____

Life-long neurogenesis is supported by populations of neural stem cells (NSCs) residing in restricted germinal regions within the adult mammalian brain (Gage,2000; Doetsch,2003). In the forebrain subventricular zone (SVZ) along the walls of the lateral ventricles, NSCs continuously generate neuroblasts that migrate to and functionally integrate as mature interneurons in the olfactory bulb (OB; Lledo et al.,2006). Once considered embryonic-like remnants of prenatal neurogenesis, adult neurogenic zones do not faithfully recapitulate the morphology and function of germinal layers. The complex architecture of the adult murine SVZ results from dynamic changes in its structure and cell type composition occurring during the first postnatal month (Alves et al.,2002; Bonfanti and Peretto,2006; Peretto et al.,2005; Tramontin et al.,2003). In this period, neuroepithelial-derived radial glial cells (Haubensak et al.,2004) change their morphological and functional features to become astrocytes of the glial tubes, which allow the migration of SVZ neuroblasts to the OB (Lois and Alvarez-Buylla,1994) (Fig. 1A). The astrocytic nature of adult SVZ primary precursors (Doetsch et al.,1999) and their origin from neonatal radial glia (Merkle et al.,2004) suggest that adult NSCs are part of a developmental lineage extending from the neuroepithelium to radial glia to germinal astrocytes, a subpopulation of which maintains life-long neurogenic competence (Bonfanti and Peretto,2006; Merkle and Alvarez-Buylla,2006; Pastrana et al.,2009). This prolonged neurogenic activity is the result of complex interactions between the primary precursors, which significantly contribute to the architecture of the niche, and the local microenvironment, which strongly influence their function

(Seaberg and van der Kooy,2002; Doetsch,2003). These interactions progressively change during the postnatal age and in adulthood, with a decrease in the number of neuroblasts and a parallel increase in the number of astrocytes, which results in increased astrocyte:neuron ratio and overt diminished neurogenesis both postnatally (Peretto et al.,2005) and during aging (Luo et al.,2006).

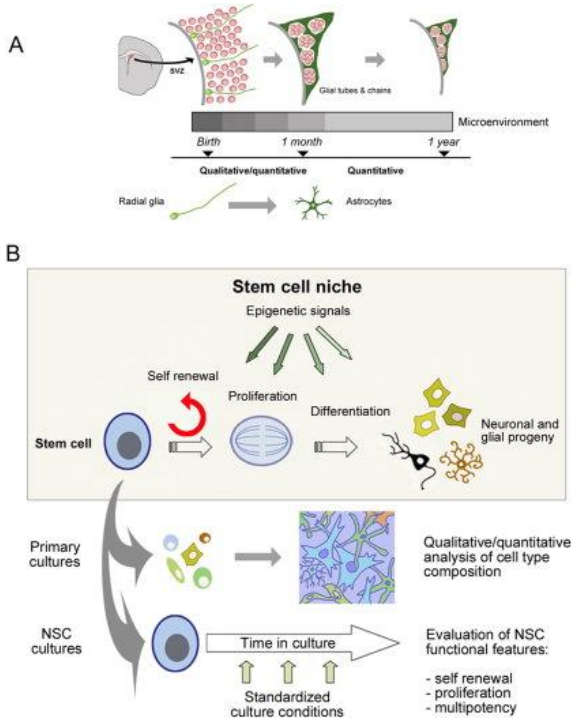

Figure 1. Stem cells/progenitors within the SVZ neural stem cell niche during postnatal brain development and after ex vivo isolation and culture. **A**: Both the anatomical and molecular environment of the SVZ neurogenic region progressively change at increasing postnatal ages in vivo, leading to formation of astrocytic glial tubes and establishment of tangential chain migration (top). In parallel with this process, a cellular transformation from radial glia to astrocytes occurs (bottom). **B**: Primary cultures and NSC cultures can be established from the SVZ neurogenic region during specific stages of postnatal brain development. In particular, the ex vivo isolation and culturing of NSC populations in standardized culture conditions allows studying their functional properties and evaluating how NSC isolation from the niche and prolonged in vitro culture might affect their proliferation, self-renewal, and differentiation potential. A magenta-green copy of this figure is available as Supplementary Figure 6.

Due to the lack of unequivocal agreement on NSC markers and to the difficulty in tracking primary precursors and their progeny in vivo, ex vivo experimental paradigms have been developed to investigate whether functional changes in NSC compartments might account for changes in neurogenic activity. Primary cultures are a widely utilized model to obtain mature cells that encompass proliferating or early postmitotic precursors. This culture system reflects the cell type composition of the tissue of origin but does not allow the ability to distinguish the contribution of stem cells versus committed progenitors to the final differentiated progeny. To overcome this limitation, models have been developed that allow ex vivo isolation and propagation of cell populations enriched in long-term self-renewing, multipotent NSCs (Gritti et al.,1999; Gage,2000; Alvarez-Buylla et al.,2002).

The experiments described herein utilize a neurosphere assay (NSA; Gritti et al.,2002; Reynolds and Rietze,2005) to isolate and culture bona fide NSC populations from the SVZ niche. This experimental program illuminates whether and to what extent the age-dependent reduction in neurogenesis observed in

vivo can be ascribed to changes in the NSC intrinsic developmental program versus (or in addition to) modifications of the niche microenvironment. To determine potential age-related functional differences, we isolated NSCs at hallmark postnatal ages where striking modifications to the SVZ neurogenic niche are apparent in vivo. Furthermore, a morphological and functional comparison of NSCs isolated from various anatomical regions within the SVZ was undertaken. While it is known that the posterior component (lateral ventricle region, LV) of the SVZ harbors the more active stem cell niche, the anterior part (rostral extension, RE) has been reported to be less active with regard to the process of adult neurogenesis. This phenomenon is likely a consequence of the early loss of direct contact with the ventricle (Doetsch et al.,2002). In addition, other groups have reported that both the age and the region are known to influence the fate of newly generated olfactory bulb neurons (Lemasson et al.,2005). Thus, in this study we evaluated the effect of age and brain region (LV vs. RE) on self-renewal, proliferation, and multipotency of NSC populations and characterized the cell type composition of NSC-derived differentiated progeny, comparing it to that of region- and age-matched primary neural cultures. In addition, we investigated the effects of culture duration to address whether NSC isolation and prolonged in vitro expansion might affect the functional properties of the cells (Fig. 1B).

This systematic and comparative analysis showed age- and region-dependent differences on the clonogenic efficiency and on the long-term proliferative capacity of NSCs. Age- and region-dependent quantitative changes (decreased quantity of neurons and oligodendrocytes; increased numbers of astroglial cells) were demonstrated in the cell composition of NSC differentiated progeny. Some of these changes were maintained in long-term cultured NSC populations. Overall, our in vitro data strengthen the hypothesis that the age- and region-dependent differences in neurogenesis observed in vivo may be ascribed to changes in the overall NSC intrinsic developmental program.

MATERIALS AND METHODS

Tissue microdissection

All animal treatments protocols were reviewed and approved by the Institutional Committee for the Good Animal Experimentation of the San Raffaele Institute (IACUC 314).

CD1 mice (Charles River, Calco, Italy) at postnatal (P) ages (P0, P5, P13, P21, P90) were anesthetized by placing the animals in crushed ice for 4 minutes (P0 and P5) or by intraperitoneal injection of Avertin (2,2,2-Tribromoethanol; Sigma-Aldrich, St. Louis, MO) (P13-P90). CD1 mice at matching postnatal ages were previously utilized to analyze the postnatal modifications of the neurogenic zones in vivo (Peretto et al.,2005) and ex vivo, using tissue explants/organotypic cultures (Canalia, Armentano, and Bonfanti, in prep.). Thus, we chose the same strain in order to assure homogeneity and comparable studies. Brains were isolated and olfactory bulbs (OB, containing the rostral part of the SVZ; RE) were removed. A coronal

slice comprising the periventricular subventricular zone (LV) was cut and the periventricular tissue was carefully dissected. Further details pertaining to tissue harvesting are found in Supplementary Figure 1.

Primary neural cultures

OB and LV tissues derived from 5–12 mice were pooled to generate each culture. Tissues were enzymatically and mechanically dissociated and primary cells were plated on 10-mm Matrigel-coated coverslips (growth factor reduced; BD Biosciences, San Jose, CA; 80,000 cells/cm2) in a chemically defined, serum and growth factor-free medium (control medium) in the presence of 2% fetal calf serum (FCS). These were cultured for 20 days (Cavazzin et al.,2005); cultures were then fixed with paraformaldehyde 4%, and finally, processed for an indirect immunofluorescence assay, as described below.

Isolation and culture propagation of NSCs

NSC cultures were established as previously described (Gritti et al.,2002). LV and RE tissues from 2–6 mice were pooled in each experiment to obtain the primary cell suspension. Primary cells were plated (2,000 cells/cm2 in T25 cm2 flasks or in multiwell plates) in control medium containing basic fibroblast growth factor (FGF2) and epidermal growth factor (EGF; Peprotech, Rocky Hill, NY; 10 and 20 ng/mL, respectively; growth medium) (Gritti et al.,2002; Cavazzin et al.,2005). Under these culture conditions a fraction of the cells proliferate to form floating clonally primary spheres (neurospheres). The number of neurospheres was counted after 7 days. Cloning efficiency was expressed as the number of primary neurospheres counted in each well/number of cells plated (20,000 cells) ×100. The total number of primary spheres/animal was calculated as: number of primary neurospheres/20,000 cells × total number of cells obtained in the primary cell suspension/number of animals from which tissues were pooled.

Growth rate and proliferation of NSCs

Seven-day-old primary spheres were collected, mechanically dissociated to a single cell suspension, and plated in growth medium (3,500 cells/cm2). This procedure was repeated twice; bulk cultures were then generated by plating cells in growth medium at a density of 104 cells/cm2. For NSC functional characterization we analyzed two to three independent NSC lines.

Cells were plated in growth medium (8,000 cells/cm2) and neurospheres were collected every 5–6 days. The total number of viable cells was assessed at each passage by Trypan Blue exclusion and growth curves were established as previously described (Gritti et al.,2002).

NSC-derived differentiated cultures

Serially passaged 5-day-old neurospheres were mechanically dissociated and single cells were plated on Matrigel-coated glass coverslips in the presence of an adhesion substrate (30,000 cells/cm2) in serum-free medium containing FGF2 (10 ng/mL). After 72 hours these cultures, which contained glial and neuronal progenitors at different stages of commitment, were exposed to serum-free medium containing 2% FCS and grown for an additional 7 days in order to achieve terminal differentiation of neural progenitors into neurons, astrocytes, and oligodendrocytes (differentiated cells). The extent of neuronal and glial differentiation/maturation was assessed using antibodies against lineage-specific markers, as described below.

Antibody characterization

Please see Table 1 for a list of all antibodies used. The Neuronal Class III β-Tubulin mouse monoclonal antibody detects a single band of ≈50 kDa in Hela and A431 lysates; these bands are blocked by the addition of the immunizing peptide (manufacturer's datasheet). In our study it stained a pattern of cellular morphology (somata and processes) that is identical to previous reports in which neuronal cells were detected in adult neural stem cell-derived cultures (Doetsch et al.,2002; Consiglio et al.,2004; Cavazzin et al.,2005).

Antigen	**Immunogen**	**Manufacturer Species Catalog no.**	**Dilution used**
Neuronal Class III β-Tubulin	Microtubules derived from rat brain	Covance (USA), mouse monoclonal, IgG2a, clone TUJ1, #MMS-435P. and rabbit polyclonal, #PRB-435P	1:500
Microtubule-associated protein MAP-2ab	Termostable fraction of bovine brain microtubules	Immunological Sciences (Rome, Italy), mouse monoclonal IgG1, clone MT-01, #MAB-10334	1:200
Galactocerebroside (GalC)	Synaptic plasma membranes from bovine hippocampus	Chemicon, (Temecula, CA, USA), mouse monoclonal IgG3, #MAB342	1:200
Nestin	Nestin purified from embryonic rat spinal cord	Chemicon (Temecula, CA, USA), rat monoclonal IgG1, clone Rat-401, #MAB353	1:200
Tenascin-C	Partially purified mouse tenascin	Sigma-Aldrich, mouse monoclonal, ascites fluid, IgG1, clone MTn-12, #T3413	1:1000
Oligodendrocyte	Homogenate of white	Chemicon, (Temecula, CA, USA), mouse	1:100

Antigen	Immunogen	Manufacturer Species Catalog no.	Dilution used
marker O4	matter of corpus callosum from bovine brain	monoclonal IgM, clone 81. Commonly referred to in the literature as monoclonal antibody O4, #MAB345	
Glial fibrillary acidic protein (GFAP)	GFAP isolated from cow spinal cord	Dako Cytomation, (Carpinteria, CA, USA), rabbit polyclonal, #Z0334	1:400
NG2 chondroitin sulfate proteoglycan	Immunoaffinity purified rat NG2 chondroitin sulfate proteoglycan	Chemicon, (Temecula, CA, USA), rabbit polyclonal, #AB5320	1:300
γ-aminobutyric acid (GABA)	GABA conjugated to BSA	Sigma-Aldrich, rabbit, affinity isolated antigen specific antibody, #A2052	1:3,000
Glutamate	Glutamate conjugated to KLH	Sigma-Aldrich, rabbit, delipidized, whole antiserum, #G6642	1:3,000
Tyrosine hydroxilase (TH)	SDS-denatured, purified recombinant rat or bovine tyrosine hydroxylase	Pel-Freez (Rogers, AR, USA), rabbit polyclonal, #P40101-0	1:200
Calbindin	Recombinant rat calbindin D-28k	Swant (Bellinzona, CH), rabbit polyclonal, #CB-38a	1:400
Calretinin	Recombinant human calretinin	Swant (Bellinzona, CH), rabbit polyclonal, #7699/4	1:400

Table 1.Primary Antibodies Used

The Neuronal Class III β-Tubulin rabbit polyclonal antibody detects a single band of ≈50 kDa in rat brain lysates. In our study it stained a pattern of cellular morphology that is identical to that obtained using the Neuronal Class III β-Tubulin mouse monoclonal antibody (confirmed by double staining using anti-MAP-2ab; present study).

The microtubule-associated protein-MAP2 antibody localizes the high-molecular-weight forms of MAP2, namely, MAP2a and MAP2b, by Western blot (WB; manufacturer's datasheet) and showed staining of somata and processes in our study (as confirmed by double staining using a rabbit Neuronal Class III β-Tubulin antibody; present study).

The galactocerebroside (GalC) detects a band of ≈75 kDa in lysates from PC12 cells (manufacturer's datasheet). It was previously shown to label Olig2-expressing neural stem cell-derived oligodendrocytes (Copray et al.,2005). The pattern of cellular morphology detected in this study is similar to that previously described in adult murine neural stem cell-derived oligodendrocytes, a fraction of them coexpressing other oligodendrocyte markers (i.e., O4; Gritti et al.,2002; Cavazzin et al.,2005; present study).

Oligodendrocyte marker O4 recognizes cell bodies and processes of premyelinating oligodendrocytes in our study, in a pattern of staining consistent with that previously reported in neural stem cell-derived immature oligodendrocytes (Copray et al.,2005), and confirmed by colabeling with anti GalC antibody (present study).

The NG2 antibody identifies both the intact proteoglycan and the 300-kDa rat NG2 core glycoprotein by WB (manufacturer's information). In our study it stained cells with the morphology of oligodendrocyte precursors and pre-oligodendrocytes, with a cellular pattern consistent with previous reports (Consiglio et al.,2004; Cavazzin et al.,2005) and further confirmed by double labeling with anti-O4 and anti-GalC antibodies (present study).

The nestin antibody was previously characterized (Hockfield and McKay,1985) to label neuroepithelial progenitor cells by immunohistochemical analysis. It recognizes a single band corresponding to nestin (200 kDa) in immunoblotting using rat brain stem tissue (Manzke et al.,2008). This antibody gave us a staining pattern as reported previously in neural precursor cells (Gritti et al.,1996; Conti et al.,2005) and in neural precursor cell-derived astrocytes in vitro (Cavazzin et al.,2005).

Tenascin-C antibody recognizes mouse Tenascin-C in glial cells and extracellular matrix of developing rodent subventricular zone tissues (Peretto et al.,2005) and in the corneal limb (Iglesia et al.,2000). Labeling is absent in Tenascin-C deficient mice (Iglesia et al.,2000). In our study the antibody stained a fraction of cells that do not coexpress the neuronal markers TUJ1 and MAP2 but can express the astrocytic marker GFAP.

The GFAP antibody recognizes the well-known intermediate filament protein expressed by astrocytes and detects a band of 51 kDa on WB of rodent brain extracts (manufacturer's technical information). In this study it stained cells with the classic morphology of fibrillary astrocytes, in a pattern of cellular staining consistent with that previously described in SVZ-derived primary astrocytes and neural stem cell-derived astrocytic progeny (Cavazzin et al.,2005).

The GABA antibody shows positive binding with GABA and GABA-KLH in a dotblot assay, and negative binding with bovine serum albumin (BSA) alone (manufacturer's technical information). This antibody labels GABAergic neurons in embryonic rat neural precursor cultures (Furmanski et al.,2009).

The glutamate antibody reacts with Glu-KLH, Glu-BSA, and KLH, but not with BSA using a dotblot immunobinding assay (manufacturer's technical information). In our study both GABA and glutamate antibodies detect a fraction of cells with neuronal morphology and coexpressing TUJ1 in both primary cultures and in NSC-derived differentiated progeny.

The tyrosine hydroxylase (TH) antibody identifies dopaminergic neurons in mesencephalic tissues and in neural stem cell-derived cultures (Sanchez-Pernaute et al.,2005; Ferrari et al.,2006). In our study it detects a fraction of cells with neuronal morphology and coexpressing TUJ1 in primary cultures.

The calbindin antibody reveals a 28-kDa band in WB of mouse brain lysates and no crossreactivity with calretinin (Chalazonitis et al.,2008).

The calretinin antibody shows no crossreaction with calbindin D-28k other Ca-binding proteins by immunoblot or immunohistochemistry on brain tissues (manufacturer's technical information). Preabsorption experiments with the antigen using the same antibody showed no specific staining (Bouilleret et al.,2000). In our study both antibodies detect a fraction of cells with neuronal morphology and coexpressing TUJ1 in both primary cultures and in NSC-derived differentiated progeny.

Immunostaining of primary and NSC cultures

Cultures were fixed in 4% paraformaldehyde, rinsed with phosphate-buffered saline (PBS), and incubated overnight at 4°C or for 2 hours at 37°C in PBS containing 10% normal goat serum (NGS), 0.3% Triton X-100 (omitted when antibodies against membrane-bound antigens were used), and appropriate single primary antibody or a combination of primary antibodies. After washing, cells were reacted for 1 hour at room temperature (RT) with the appropriate secondary antibodies. For double staining, a combination of two indirect immunofluorescence procedures with Alexafluor488 and Alexafluor546-conjugated antibodies (1:2,000, Molecular Probes, Eugene, OR) was used. Samples were rinsed three times with PBS, once with distilled water, and mounted with Fluorsave (Calbiochem, La Jolla, CA). Nuclei were counterstained with 4,6-diamine-2-phenylindole dihydrochloride (DAPI; Sigma) for 5 minutes at RT. Negative control samples included: 1) mouse embryonic fibroblasts; 2) NSC differentiated cultures in which primary antibodies were omitted.

Samples were visualized with: 1) a Nikon Eclipse E600 epifluorescence microscope; images were acquired using a Nikon DMX 1200 digital camera and ACT-1 acquisition software (Nikon); 2) a Zeiss Axioskop2 microscope using double laser confocal microscopy with a Zeiss Plan-Neofluar objective lens (Zeiss, Arese, Italy); images were acquired using a Radiance 2100 camera (Bio-Rad, Segrate, Italy) and LaserSharp 2000

acquisition software (Bio-Rad). Confocal images were imported into Adobe Photoshop software (San Jose, CA) without modifications in brightness/contrast. Five fields/coverslip were counted (800–1,000 cells/coverslip), 2–16 replicates for each antigen in 2–3 independent experiments. Data are expressed as percentages of cells displaying immunoreactivity for each specific antigen (number of immunoreactive cells/total number of cells × 100). Levels of MAP2 and TUJ1 coexpression are expressed as number of TUJ1+MAP2+ cells/total TUJ1+ cells.

Statistical analysis

One-way and two-way analysis of variance (ANOVA) followed by Tukey's or Bonferroni's multiple comparison test were employed to compare percentages of immunoreactive cells. For growth curves, data were interpolated using a linear regression model and best fitted the following equation: $y = a + bx$, where y is the estimated total number of cells (in log scale), x is the time (DIV), a is the intercept, and b is the slope. The best-fit value, the standard error, and the 95% confidence intervals of the slope for each dataset were calculated. The slope values were then compared using one-way ANOVA followed by Bonferroni's multiple comparison test (slope values of NSC lines for each brain region) or by F test (slope values of SVZ and OB NSC lines for each age). Statistical significance was accepted with $P \leq 0.05$.

RESULTS

Cell type composition of primary neural cultures display age- and region-dependency

Primary neuronal and glial mixed cultures were obtained by plating cells freshly isolated from the LV and OB tissues in adhesion, in a growth factor-free medium containing 2% FBS. In this experimental setting we considered the whole OB, since both the RE- and non-RE OB tissue contribute to the culture (Suppl. Fig. 1). Three weeks after plating the cell type composition was assessed using an immunofluorescence analysis. Immature and mature neurons were identified by means of TUJ1 and MAP2 immunoreactivity (IR), respectively. Astrocytes were identified based on GFAP IR. Immature neuroepithelial cells and cells expressing radial glia features were identified by Nestin and Tenascin-C (Ten-C) IR. Immature oligodendrocyte precursors, pre-oligodendrocytes, and nonmyelinating oligodendrocytes were identified based on NG2, O4, and GalCer IR, respectively.

Within the neuronal population we observed a significant age-dependent decrease in the proportions of LV-derived TUJ1+ neurons as age increased as well as a moderate but significant region-dependent effect (Fig. 2A,B). Also, significantly lower numbers of MAP2+ with respect to TUJ1+ cells were detected in LV-derived cultures, with no significant age-dependent effect. In OB-derived cultures the percentages of both TUJ1+ and MAP2+ neurons did not show significant age-dependent changes (Fig. 2B) and significant lower percentages of MAP2+ versus TUJ1+ neuron were observed only in P0 and P13 cultures (see figure legends

for details on statistical analysis). In LV-derived cultures, TUJ1+ cells displayed mainly bipolar morphology (Fig. 2C–E). In neonatal cultures, MAP2 was expressed in 50–70% of the TUJ1+ cells (Fig. 2I). In cultures >P13 virtually all MAP2+ neurons maintained TUJ1-IR and displayed long, thin processes and varicosities (Fig. 2J). In contrast, OB-derived TUJ1+ cells at any postnatal age were mainly multipolar, with long processes forming a wide and intricate network (Fig. 2F–H). In late postnatal and adult cultures, TUJ1+MAP2+ neurons had long processes and were morphologically and topographically distinct from TUJ1+MAP2− neurons, which were characterized by long processes laying side-by-side or the top of glial cells (Fig. 2K,L). Neuronal subtypes known to characterize LV-derived glomerular and periglomerular OB neurons (Kohwi et al.,2007) were present in LV- and OB-derived cultures, with both region- (for GABA+ and TH+ cells) and age-dependent differences (for calretinin+ and calbindin+ cells) (Suppl. Fig. 2). Overall, these results indicate an age-dependent loss of neurogenic capacity, particularly evident in LV-derived cultures, and suggest a more mature phenotype in the OB neuronal population compared to the LV counterpart.

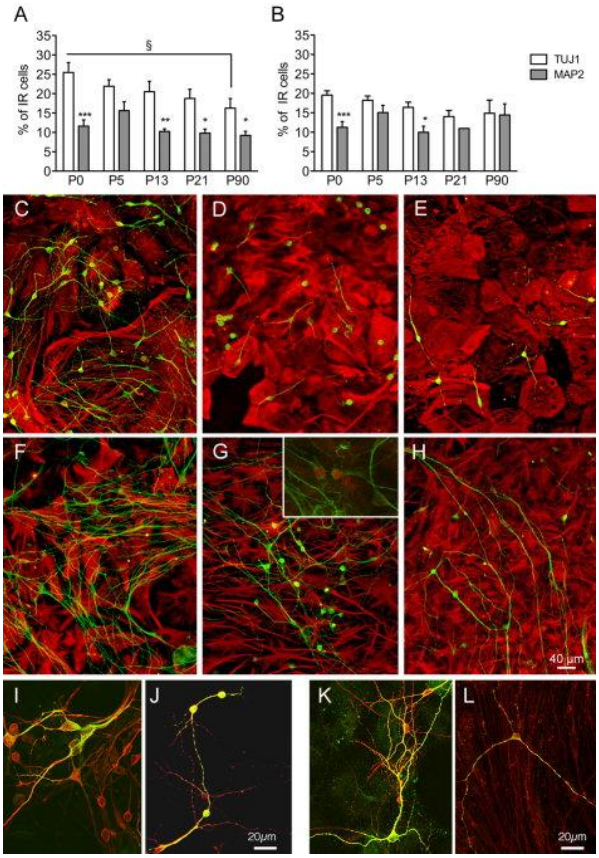

Figure 2. Age- and region-dependent changes in the neuronal cell population in primary cultures derived from different regions of the SVZ niche. A: In LV cultures we observed a significant age-dependent decrease of the TUJ1+ cell population (2-way ANOVA: F = 2.69; DFn = 4 DFd = 86; P = 0.0362; one-way ANOVA followed by Bonferroni's multiple comparison test for age-related changes for each marker: P0 vs. P90 §P <0.05) as well as a moderate but significant region-dependent effect (2-way ANOVA: F = 6.70; DFn = 1 DFd = 86; P = 0.013; Bonferroni posttests: LV vs. OB P <0.05 at P0 and P5, not significant at all other ages; compare white columns in A,B). Significant lower numbers of MAP2+ with respect to TUJ1+ cells were detected, with no significant age-dependent effect (2-way ANOVA: F = 25.37; DFn = 4 DFd = 76; P <0.0001; Bonferroni posttest: *P <0.05, **P <0.01, ***P <0.001). B: In OB-derived cultures the percentages of both TUJ1+ and MAP2+ neurons did not show significant age-dependent changes and significant lower percentages of MAP2+ vs. TUJ1+ neuron were observed only at P0 and P13 (2-way ANOVA, F = 10.04; DFn = 1 DFd = 53; P = 0.0025. Bonferroni posttests: TUJ1 vs. MAP2 ***P <0.001 and *P <0.05). Data are from 3–5 independent experiments, for a total of 3 to 16 replicates for each treatment; bars represent the standard error of the mean. LV cultures (C–E) and OB age-matched counterpart (F–H) showed peculiar neuronal and astroglial

morphology. C,F: P0; D,G: P13; E,H: P90. Neurons (TUJ1), green; astrocytes (GFAP), red. Inset in G: proliferating neuroblasts (Ki67, red; TUJ1, green). I–L: Confocal pictures showing neurons coexpressing TUJ1 (red) and MAP2 (green) in LV cultures (I, P0; J, P90) and OB cultures (K, P0; L, P90). Yellow/orange color indicates merged signal. A magenta-green copy of this figure is available as Supplementary Figure 7. Scale bars = 40 µm in C–H; 20 µm in I–L.

The proportions of GFAP+ astroglial cells in LV- and OB-derived late postnatal and adult primary cultures showed a moderate (1.6-fold) but significant age-dependent increase (Fig. 3A). We identified subpopulations of cells expressing radial glia/immature neuroepithelial cell markers, e.g., nestin (Fig. 3B) and Tenascin-C (15–30% and 6–15% of the total number of cells in culture). Nestin-expressing cells displayed distinct morphology depending on both the age and the region of origin of the cultures and a variable fraction of them coexpressed GFAP (Fig. 3C–E). A decrease in the proportion of neurons and increase in the proportions of astroglial cells affected the neuron:astrocyte ratio, which was about 1:1 (TUJ1) and 1:2 (MAP2) in P0, P5, and P13 cultures and changed in favor of astrocytes in cultures from older ages (1:4 for TUJ1 in P90 LV cultures) (Fig. 3F). This trend was similar but less evident in OB-derived cultures (Fig. 3D). On the contrary, the ratio between the proportions of TUJ1+ and MAP2+ neurons was stable in all the cultures (Fig. 3F,G).

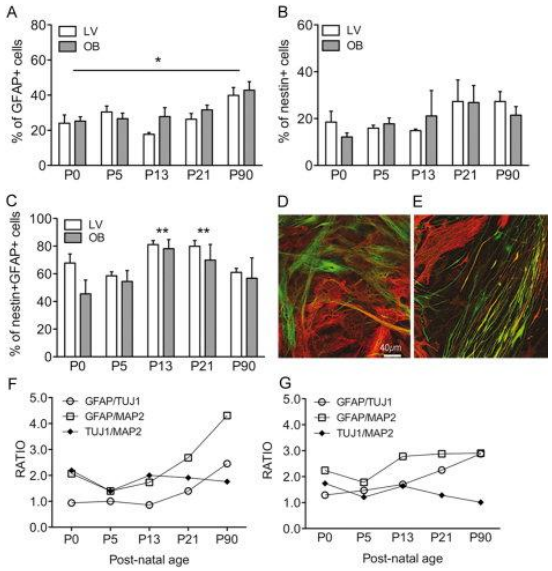

Figure 3. Glial populations in primary cultures derived from different regions of the SVZ niche. A: The proportions of GFAP+ astroglial cells showed an age-dependent increase (2-way ANOVA, F = 7.72. DFn = 1 DFd = 88, P <0.0001; one-way ANOVA followed by Bonferroni's multiple comparison test for age-related changes for each region, *P <0.05 for both LV and OB), but no significant region-dependent changes (2-way ANOVA, F = 1.82. DFn = 4 DFd = 88, P = 0.1812). B: The proportions of nestin+ cells were not significantly affected by the age (2-way ANOVA, F = 1.71. DFn = 4 DFd = 23, P = 0.1826) or by the region considered (2-way ANOVA, F = 0.07. DFn = 1 DFd = 23, P = 0.797). C: The number of GFAP+nestin+ showed a significant age-dependent change, with a peak at P13–P21 (2-way ANOVA, F = 4.67. DFn = 4 DFd = 17, P <0.01; Bonferroni posttests: **P <0.01), with not quite significant differences with respect to the brain region (2-way ANOVA, F = 3.63. DFn = 1 DFd = 17, P = 0.073). D,E: Double immunofluorescence followed by confocal analysis revealed polygonal and fibrous morphology of nestin+ cells in LV (D) and OB (E) cultures, respectively. Note the presence of GFAP+nestin+ cells in both cultures (GFAP, red; nestin, green. Yellow/orange color indicates merged signal). F,G: Age-dependent increase of the astrocyte:neuron ratio in LV (F) and OB (G) primary cultures. The ratio between immature (TUJ1) and mature neurons (MAP2) was stable. Data are from 3–5 independent experiments, for a total of 3–12 replicates for each treatment; bars in A–C represent the standard error of the mean. Scale bar = 40 µm (D,E). A magenta-green copy of this figure is available as Supplementary Figure 8.

Similar to neurons, the number of NG2+, GalCer+, and O4+ oligodendroglial cells showed a significant age-dependent decrease (60–80% reduction in adult with respect to neonatal cultures), but not a significant region-dependent change for each marker considered (Suppl. Fig. 3A–E). Progenitor cells (NG2+) coexpressing O4 or GalCer were present in variable proportions in all cultures, indicating the acquisition of a mature phenotype eventually results in the loss of the immature marker (Suppl. Fig. 3F–H).

NSCs and their progeny display age- and region-dependent functional heterogeneity

In order to clarify whether the quantitative (decreased numbers of TUJ1+ neurons and oligodendrocytes, increased numbers of GFAP+ astrocytes) and qualitative (different cell morphology) differences observed in primary cultures might be ascribed to age- and region-dependent changes in the functional properties of the stem/early precursor cell compartment, bona fide NSCs were isolated and expanded from age-matched LV and OB tissues using the neurosphere assay (NSA) (Reynolds and Rietze,2005). Under these stringent culture conditions, only the RE tissue in the OB contains sphere-forming cells (Gritti et al.,2002; Suppl. Fig. 1). Thus, we will hereafter refer to this region as RE.

We showed a significant age- and region-dependent decrease in the number of primary neurospheres that could be retrieved from tissue (15,318.0 ± 691.9 and 404.8 ± 44.9 neurospheres/animal for LV; 5,650.0 ± 587.3 and 39.1 ± 5.2 neurospheres/animal for RE at P0 and P90, respectively; mean ± SEM, 2 or 3 independent experiments, 3 replicates/experiment). The cloning efficiency (CE; an index of the number of sphere-forming cells present in the primary cell suspension) of LV and RE primary cells showed a 3-fold and an 8-fold decrease, respectively, from P0 to P90. Also, RE primary cells showed a 3–6-fold decrease of CE in comparison to the LV counterparts at all ages considered (Fig. 4A). We harvested and serial dissociated primary neurospheres, establishing NSC lines from all the samples. All NSC lines displayed stable long-term proliferation and self-renewal up to 15 subculturing passages (the longest timepoint considered), regardless of the region and the age of the tissue of origin, although the lines displayed differences in the expansion rate (increase in cell number ranged from 2–6 logs; subculturing passages 2–8 are shown in Fig. 4B–H). Postnatal and adult-derived LV NSC lines (P13, P21, and P90; Fig. 4B,F–H) displayed a modest age-dependent decrease in growth rate compared to neonatal and early postnatal-derived counterparts (P0 and P5; Fig. 4B,D,E). While the growth rate of neonatal LV- and RE-derived NSC lines was similar (Fig. 4D), we observed a significant drop in the growth rate of RE NSC lines derived at all other ages with respect to the neonatal counterpart and a significantly decreased growth rate of ≥P5 RE cell lines compared to the age-matched LV counterparts (Fig. 4E–I).

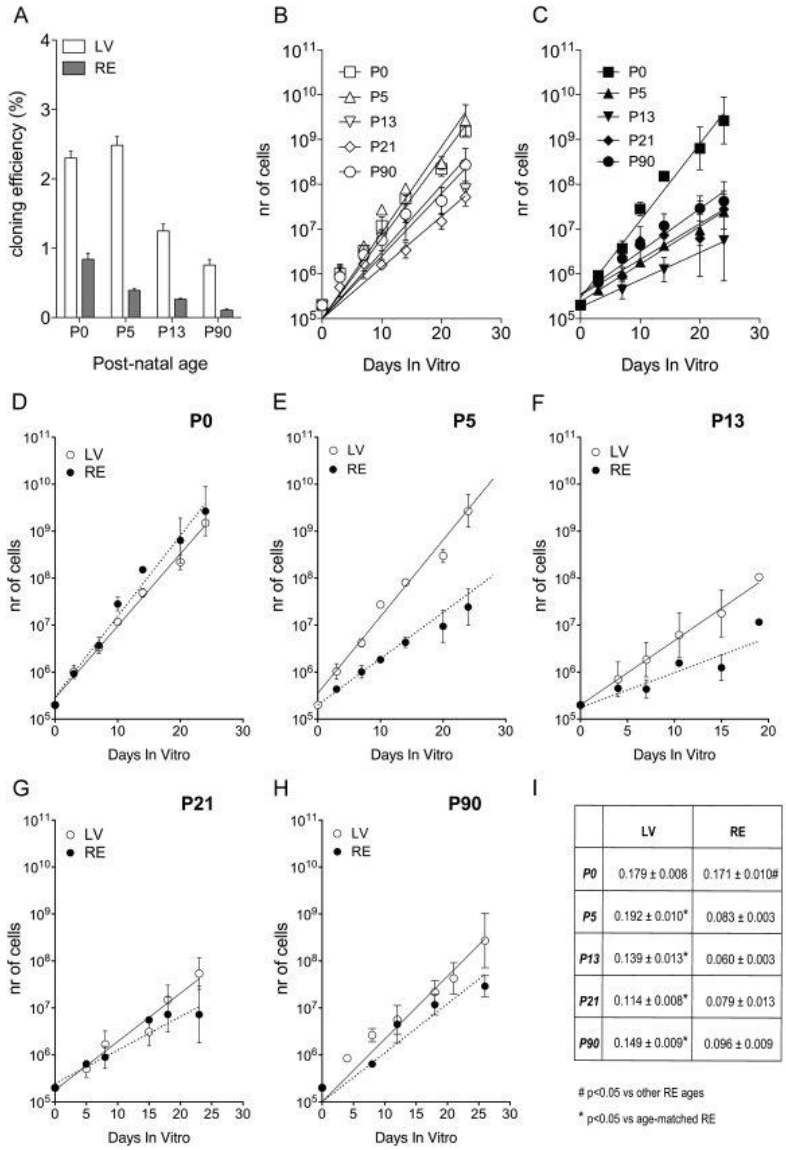

Figure 4. Proliferation and self-renewal of NSCs derived from LV and RE tissues at different postnatal ages. A: Age- and region-dependent differences in the number of primary neurospheres generated by means of the NSA. Data shown in the graph indicate a significant age-dependent decrease in cloning efficiency (CE) for both LV- and RE-derived primary cells (2-way ANOVA F = 93.86. DFn = 3 DFd = 40, P <0.0001; one-way ANOVA followed by Bonferroni's multiple comparison test: P0 and P5 vs. P13 and P90 P <0.0001; P13 vs. P90 P <0.05) as well as a significant region-dependent effect on CE, which is decreased in the RE- with respect to LV-derived cultures (2-way ANOVA F = 532.97. DFn = 1 DFd = 40 P <0.0001; Bonferroni posttests: LV vs. RE P <0.0001 at all ages). Moreover, the region-dependent variation does not have the same effect on the CE at all values of age (2-way ANOVA F = 31.04. DFn = 3 DFd = 40 P <0.0001). CE is expressed as number of neurospheres obtained/number of cells plated 100×. Data are expressed as the mean ± SEM. Tissues coming from 2–6 mice were pooled in each experiment to obtain the primary cell suspension that was plated in triplicate. n = 2 independent experiments. B,C: NSC lines established from the LV (B) and RE (C) at different postnatal ages displayed long-term proliferation and self-renewal (subculturing passages 2 to 8 are shown in the graphs). D–H: Comparison of LV- and RE-derived stem cell lines at each age showed increased growth rate of LV-derived lines with respect to the age-matched RE-derived counterparts, except for NSC derived from P0 tissues (in which this trend is reversed) and P21. Each point of the growth curves represents the mean ± SEM of n = 3 independent LV and RE NSC lines. Data were interpolated using a linear regression model and best fitted the following equation: y = a + bx, where y is the estimated total number of cells (in log scale), x is the time (days in vitro, DIV), a is the intercept, and b is the slope. Regression lines are shown in the graphs as continuous and dotted lines for LV- and RE-derived NSC lines, respectively. I: Slope values (b) ± SEM for NSC lines derived from LV and RE at the different postnatal ages.

As proliferation and self-renewal are necessary but not sufficient to identify a population of cells as containing stem cells (Reynolds and Rietze,2005), we evaluated multipotentiality in LV and RE-derived NSCs at early (3rd) and late (10th) subculturing passages. This was completed in order to verify the long-term capability of differentiation into astrocytes, neurons, and oligodendrocytes and to test the effects of culture duration on this property.

Early-passage NSCs.

The neuronal population exhibited a significant age-dependent decrease in the total number of TUJ1+ cells derived from both regions (2–3-fold decrease in P90 versus P0 differentiated cultures and a significant but smaller effect was observed in the MAP2+ cell population; Fig. 5A, LV; Fig. 5B, RE). Also, significantly lower numbers of TUJ1+ neurons were found in neonatal/early postnatal cultures RE cultures with respect to the LV counterparts (Fig. 5A,B). Interestingly, TUJ1+ neurons were most numerous as compared to MAP2+ neurons in neonatal LV and RE cultures. In LV-derived cultures the large majority of TUJ1+ neurons showed bipolar morphology (Fig. 5E–G). Since all MAP2+ neurons maintained TUJ1-IR, levels of TUJ1 and MAP2 coexpression decreased in LV-derived cultures at increasing ages (P0: 76.44 ± 4.31%; P5: 70.59 ± 10.52%; P13: 51.90 ± 9.13%; P21: 54.95 ± 1.45%; P90: 35.95 ± 11.12%), while they were stable in RE-derived cultures (P0: 67.55 ± 15.13%; P5: 73.64 ± 5.03%; P13: 67.75 ± 11.53%; P90: 82.56 ± 7.87%; mean ± SEM, n = 3 independent experiments, 3 replicates/experiment). The morphology of RE-derived primary neurons resembled that observed in OB primary cultures, while astrocytes displayed a flat and polygonal morphology (Fig. 5H–J).

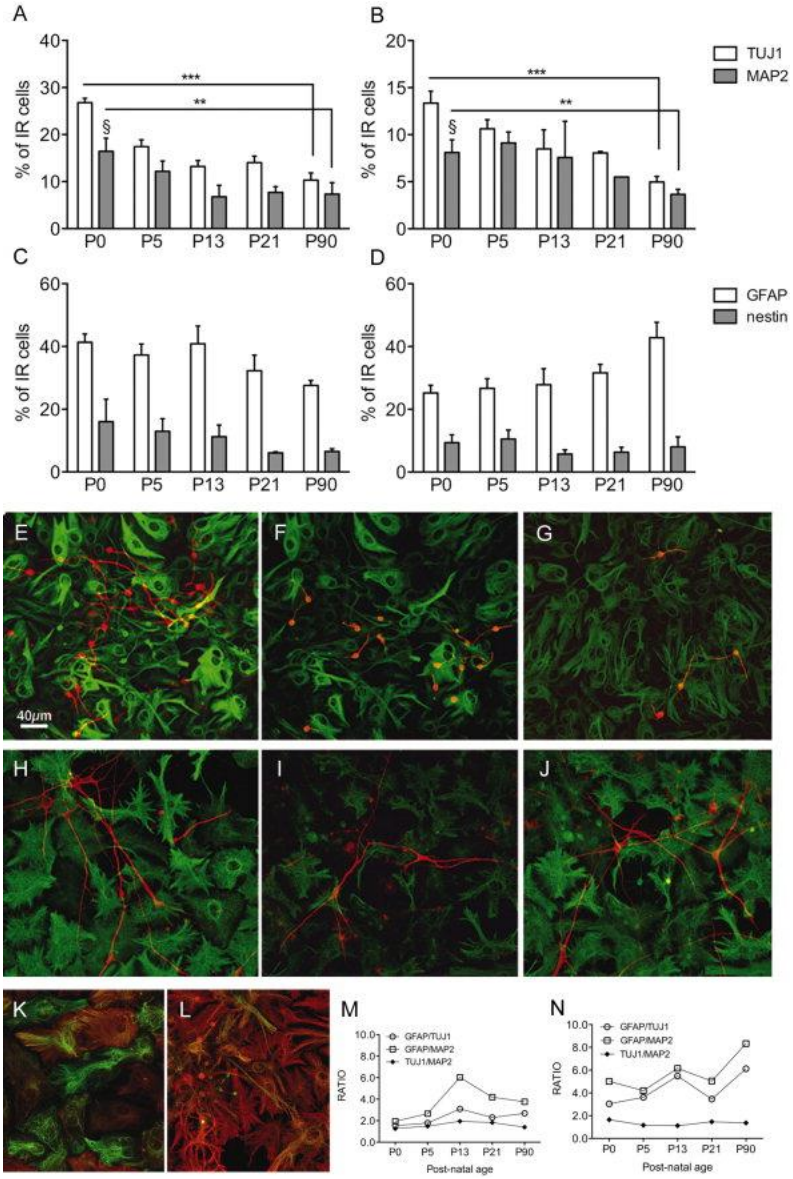

Figure 5. Neuronal and glial populations in early passage NSC progeny. A,B: A significant age-dependent decrease in the number of TUJ1+ and MAP2+ cells was found in LV- (A; 2-way ANOVA F = 15.27. DFn = 4 DFd = 32 P <0.0001) and RE- (B; 2-way ANOVA F = 3.74. DFn = 4 DFd = 28 P <0.05) differentiated cultures. One-way ANOVA followed by Bonferroni's multiple comparison test performed for age-related changes for each marker **P <0.01, ***P <0.001). RE cultures showed significant lower numbers of TUJ1+ neurons with respect to the LV counterparts at all ages considered (compare white bars for matched ages in A and B; 2-way ANOVA F = 62.97. DFn = 1 DFd = 42, P <0.0001). A significant region-dependent decrease in the numbers of MAP2+ cells with respect to TUJ1+ cells was observed at P0 in LV- (2-way ANOVA F = 27.70. DFn = 1 DFd = 32, P <0.0001; Bonferroni posttests §P <0.05) and OB- (2-way ANOVA F = 3.82. DFn = 1 DFd = 28, P = 0.05; Bonferroni posttests §P <0.05). C,D: The proportions of GFAP+ and nestin+ cells were stable in LV- and RE-derived cultures as a function of age. A significant region dependent difference was observed for GFAP+ cells only at P0 and P90 (compare white bars for matched ages in C,D; 2-way ANOVA F = 4.34. DFn = 1 DFd = 75, P = 0.0406; Bonferroni posttests: LV vs. RE at P0 and P90 P <0.05). E,F: Morphology of neurons (TUJ1, red); and astrocytes (GFAP, green) in LV (E–G) and RE-derived NSC cultures (H–K) at different ages (E,H: P0; F,I: P13; G,J: P90). Data in A–D are from 3–5 independent experiments, for a total of 3–5 replicates for each treatment; bars represent the standard error of the mean. K,L: Confocal pictures show a fraction of nestin+ cells coexpressed GFAP in both LV- (K) and RE- (L) derived cultures (green, nestin; red, GFAP; yellow-orange color indicates merged signal). Age-dependent increase of the astrocyte:neuron ratio in LV (M) and, more evident, in RE-derived NSC cultures (N). The ratio between immature (TUJ1) and mature neurons (MAP2) was stable. A magenta-green copy of this figure is available as Supplementary Figure 9. Scale bar = 40 μm for A–L.

Since proportions of GFAP+ astrocytes were fairly stable in cultures at increasing ages (Fig. 5C, LV; Fig. 5D, RE), the neuron (TUJ1) : astrocyte (GFAP) ratio was about 1:2 (LV) and 1:4 (RE) in P0 cultures and increased 2–3-fold in cultures from older ages. On the contrary, the ratio between the proportions of TUJ1+ and MAP2+ neurons remained stable (Fig. 5M,N). Also, in all the NSC-derived differentiated cultures we identified cells expressing nestin (5–10% of the total number of cells, Fig. 5C,D) and Ten-C (1–5% of the total number of cells; not shown). The proportions of these populations did not differ significantly in RE- and LV-derived cultures (Fig. 5M,N). Only a fraction of nestin and Ten-C-expressing cells coexpressed GFAP; thus, the different combination of the two markers identified distinct glial subpopulations. GFAP+nestin+ cells represented 20–60% of the total number of GFAP+ cells and this was dependent on the age and region considered. Most of this population resembled the typical flat and polygonal astrocytes but differed from the small fraction of nestin+GFAP− bipolar cells (Fig. 5K, LV; Fig. 5L, RE). Ten-C+ cells were mainly bipolar, with small soma and short processes and rarely coexpressed GFAP. The rare Ten-C+GFAP+ cells showed glial-like morphology and expressed the protein in the soma, often in a vesicular localization (data not shown).

Overall, these results indicate that NSCs cultured for a limited period of time (three subculturing passages) in vitro showed age- and region-dependent quantitative differences in the neuronal cell population that resembled those found in age- and region-matched primary cultures. However, only if criteria of long-term proliferation, self-renewal, and multipotency are satisfied can we attribute those functional differences to the stem cell compartments that are maintained within the bulk-passaged cell populations. For this reason, we repeated our analysis on NSC populations grown for 10 subculturing passages.

Late-passage NSCs.

Consistent with results obtained in early cultures, the proportion of neurons showed a 1.5–2-fold decrease in LV (Fig. 6A) and RE (Fig. 6B) NSC cultures derived from adult tissue with respect to those derived from neonatal tissues. This affected both TUJ1+ and MAP2+ cells but was less evident in RE NSC. When comparing 3rd and 10th-passage LV-derived cultures, we found a significant (up to 50%) reduction in the number neurons in late-passage cultures. This was particularly evident in neonatal (TUJ1+ cells: 26.80% ± 0.98% and 16.54% ± 1.19% in P0 early and late cultures, respectively) with respect to adult-derived cultures (TUJ1+ cells: 10.30% ± 1.53% and 7.15% ± 0.94%; P90 early and late cultures, respectively; compare Figs. 5A and 6A; see also Suppl. Fig. 5 and Suppl. Table 1 for statistics). Differential morphology remained evident in 10th-passage RE-derived neurons (Fig. 6F–H) with respect to the LV counterpart (Fig. 6C–E). GABA+ and glutamate+ cells were the most abundant in NSC-derived cultures (5–30% of the total number of cells, with variability depending from the postnatal age). Calbindin+ and calretinin+ cells accounted for 3% or less of the total number of cells in cultures and no TH+ neurons were observed (Suppl. Fig. 4).

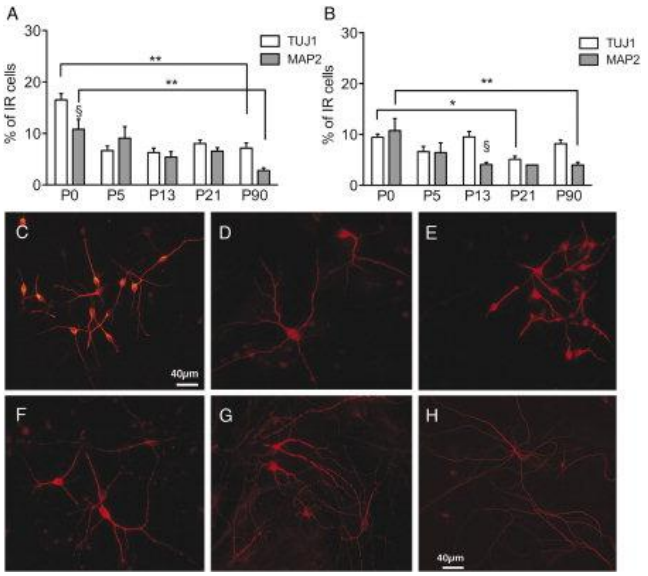

Figure 6. Neuronal population in late-passage NSC cultures. A,B: The proportion of TUJ1+ and MAP2+ neurons showed a significant age-dependent decrease in both LV- (A; 2-way ANOVA F = 11.76. DFn = 4 DFd = 63, P <0.0001) and RE-derived cultures (B; 2-way ANOVA F = 3.65. DFn = 4 DFd = 34, P = 0.0141). **P <0.01, *P <0.05; one-way ANOVA followed by Bonferroni's multiple comparison test performed for age-related changes for each marker. A region-dependent difference in the numbers of TUJ1+ cells was observed only in P0 LV cultures (compare white bars in A,B; Bonferroni posttests P <0.05) and a significant decreased proportions of MAP2+ as compared to TUJ1+ cells was evident at P0 (LV) and P13 (RE) (Bonferroni posttests: §P <0.05). A peculiar neuronal morphology distinguished RE-derived cultures (F, P0; G, P13; H, P90) from their LV counterpart (C, P0; D, P13; E, P90) at any age considered. Scale bars = 40 µm (C–H). A magenta-green copy of this figure is available as Supplementary Figure 10.

The proportion of 10th-passage NSC-derived GFAP+ cells showed a significant increase only in P90 cultures (Fig. 7A). Glial progeny showed flat protoplasmic morphology, irrespective of the region and age considered (Fig. 7B–D). When comparing 3rd and 10th-passage cultures, we found a significant increase in the number of GFAP+ cells in ≥P21 late-passage LV and RE-derived cultures (see Suppl. Fig. 4 and Suppl. Table 1 for statistics). Similar proportions of nestin+ cells in 3rd and 10th-passage cultures were observed, with no differences with respect to the region considered (data not shown). Consistent with our previous observations a fraction of nestin+GFAP+ cells (30–50% of the total number of GFAP+ cells) showed the typical flat polygonal morphology. Few nestin+GFAP− cells showed fibrous morphology with thin processes (Fig. 7B,C, LV; Fig. 7D,E, RE) and no Ten-C-expressing cells were identified. The relative neuron:astrocyte ratio increased from 1:3 (LV) and 1:4 (RE) of P0 cultures up to 1:10–1:20 in adult cultures (Fig. 7F, LV; Fig. 7G, RE).

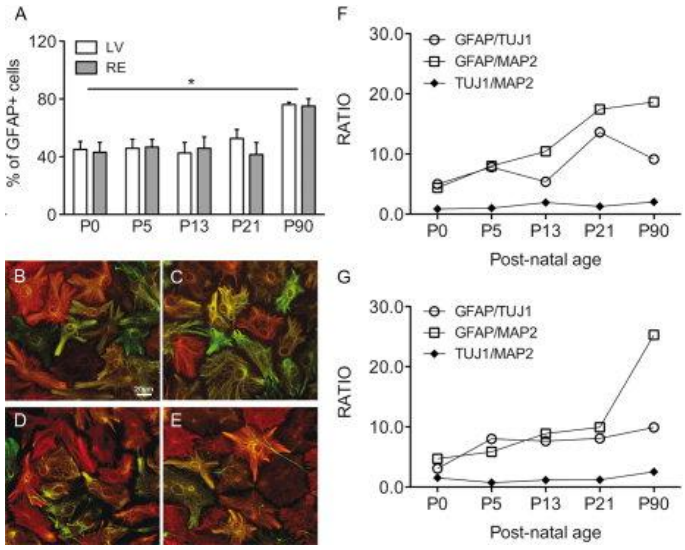

Figure 7. Glial population in late-passage NSC cultures. A: Significant age-dependent increase of GFAP+ cells in LV- and RE-derived cultures (2-way ANOVA F = 5.95. DFn = 4 DFd = 80, P = 0.0003), without region-dependent effects (2-way ANOVA F = 0.15. DFn = 1 DFd = 80, P = 0.698). *P <0.05 one-way ANOVA followed by Tukey's multiple comparison test for age-related changes for each region. B–E: GFAP+ astrocytes (red) showed similar morphology irrespective of the region (LV, B,C; RE, D,E) and age considered (P0, B,D; P21, C,E); 30–50% of the total number of GFAP+ cells expressed nestin (green). The majority of GFAP+nestin+ showed polygonal morphology. Only rare nestin+GFAP− cells showed stellate morphology with thin processes. Green, nestin; red, GFAP; yellow/orange color indicates merged signal. F,G: Age-dependent increase of the astrocyte:neuron ratio in LV (F) and RE-derived (G) NSC differentiated cultures. The ratio between immature (TUJ1) and mature neurons (MAP2) was stable. Data are from 3–5 independent experiments, for a total of 3–10 replicates for each treatment; bars represent the standard error of the mean. Scale bar = 20 μm (B–E). A magenta-green copy of this figure is available as Supplementary Figure 11.

Diminishing proportions of oligodendroglial progenitor cells in NSC-derived cultures as a function of postnatal ages (Fig. 8A,B) were observed. Progenitors (NG2+) coexpressing O4 or GalCer were present in variable proportions in all the cultures (Fig. 8E–G). When comparing 10th with respect to 3rd passage NCS cultures only a few significant differences were observed (see Suppl. Fig. 5 and Suppl. Table 1).

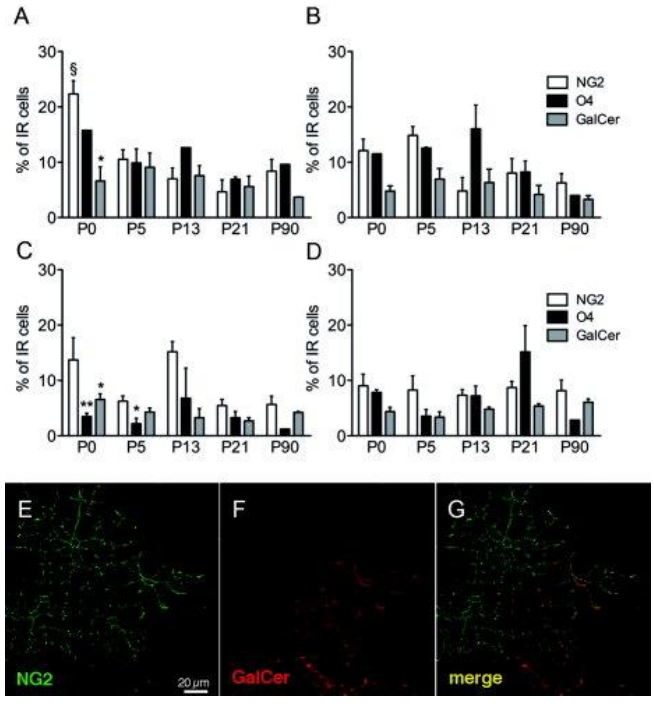

Figure 8. Oligodendroglial cells in early and late passage NSC cultures. A–D: A significant age-dependent decrease in the number of NG2+ progenitors was observed in early-passage LV-derived (A; 2-way ANOVA F = 11.16. DFn = 4 DFd = 27 P <0.0001; Bonferroni posttests. *P <0.05 **P <0.01 NG2 vs. GalCer and O4; one-way ANOVA followed by Tukey's multiple comparison test for age-related changes: §P <0.05 P0 vs. other ages) but not RE-derived cultures (B). Numbers of pre-oligodendrocytes (O4+) and nonmyelinating oligodendrocytes (GalCer+) did not show significant age- or region-dependent differences in either early- and late-passage cultures. Percentages of oligodendroglial cells do not decrease significantly in 10th (C,D) vs. 3rd passage (A,B) NSC cultures (see Suppl. Fig. 4 and Table 1 for statistics). Data are from 3–4 independent experiments, for a total of 2–5 replicates for each treatment; bars represent the standard error of the mean. E–G: Cells coexpressing NG2 (E) and GalCer (F) were present in variable proportions in all the cultures, indicating the presence of cells at different stages of differentiation/maturation. Representative confocal pictures taken from P13 LV cultures are shown. NG2, green; GalCer, red. Yellow/orange color indicates merged signal. A magenta-green copy of this figure is available as Supplementary Figure 12. Scale bar = 20 μm.

DISCUSSION

The study described herein examines the occurrence and extent of potential functional changes of the endogenous stem/precursor cell compartments and whether these changes contribute to the age-dependent alterations in the neurogenic activity in the various regions of the SVZ neurogenic niche in vivo. We performed a systematic analysis on neural stem cell lines (Reynolds and Weiss,1992; Gritti et al.,2002) established from tissues isolated from the LV region and the RE region of the SVZ throughout postnatal development. The aim was to clarify: 1) which NSC/progenitor features are cell-intrinsic and which might depend on the environment that undergoes temporal (different postnatal ages)- and spatial (anatomical region)-dependent changes; 2) how NSC isolation from the niche and their prolonged in vitro culture might affect their pattern of cell proliferation and differentiation potential. We compared neural stem cell lines with a complementary in vitro model, i.e., mixed primary cultures, which mirror the cell type composition of the tissue from which they are established.

The main findings are: 1) the postnatal age and the SVZ region from which stem/progenitor cells are isolated (LV vs. RE) significantly impact their clonogenic activity and their pattern of long-term proliferation (albeit this was stable in culture); 2) the proportion of neurons that differentiate (short- and long-term cultured NSCs) significantly decrease as a function of the postnatal age of the tissue of origin. Importantly, the age-dependent decrease in neurogenic activity, as well as the regional differences in the relative proportion of neuronal and glial cells, closely resembles those found in age- and region-matched primary cultures; 3) decreased number of neurons are generated from long- with respect to short-term passaged NSCs.

Age- and region-dependent pattern of long-term proliferation in ex vivo isolated neural stem/progenitor cell populations

In primary cultures the contribution of progenitors and stem cells to the terminal differentiated progeny cannot be distinguished. For this reason, we applied the NSA to isolate, expand, and enrich in vitro a population of NSCs and early progenitor cells on which we verified long-term self-renewal and multipotency (Gritti et al.,2002; Reynolds and Rietze,2005).

We observed significant region- and age-dependent differences in the recovery of primary neurospheres in culture. The age-dependent decline of clonogenic efficiency in the LV region is in agreement with the age-dependent reduction of transit amplifying cells observed in vivo (Maslov et al.,2004; Luo et al.,2006). In fact, while both primary precursors and their proliferative progeny can function as NSCs in vitro when exposed to mitogens (Gritti et al.,1999; Doetsch et al.,2002), activated astrocytes and transit-amplifying cells are responsible for the majority of the primary neurospheres obtained in vitro (Reynolds and Rietze,2005; Pastrana et al.,2009). Our data is the first demonstration that this is the case for precursors residing in the RE region. In addition, we documented a significant decrease in neurosphere-forming ability of precursors isolated from the RE-derived precursors as compared to those from the LV region of the SVZ niche throughout development.

Given that stem cells have a greater self-renewal potential than nonstem cells (Seaberg and van der Kooy,2002,2003), serial passage data on bulk cultures more accurately reflect NSC frequency than data based solely on neurosphere formation (Reynolds and Rietze,2005). Thus, age- and region-dependent differences in cell expansion that we observe in our bulk population (analysis performed over eight subculturing passages, >50 days in culture) might be more correctly ascribed to differences in the size and/or in the function of long-term proliferating cells that make up the NSC compartments in those populations. While we showed moderate age-dependent decrease in the growth rate of LV-derived NSC lines, we documented a reduced expansion of RE-derived NSCs with respect to their LV counterparts. These results extend our previous findings obtained with adult cultures (Gritti et al.,2002). The only exception was found in P0 NSC bulk cultures, where a robust growth rate coupled with lower numbers of primary neurospheres in RE versus LV tissues was observed. This may reflect lower numbers of proliferative progenitors and a small NSC compartment with high self-renewal/proliferative potential in the neonatal olfactory ventricle, which is still open at birth. The significant decrease of primary neurosphere numbers and of the growth rate at older ages indicates both reduced numbers of residing precursors and changes in their functional properties after the ventricle closure, which is complete within the first 5 postnatal days (Peretto et al.,2005; Bonfanti and Peretto,2006). These data also support the theory that NSCs do require a direct contact with the ventricular lumen to actively exert their functional properties within the stem cell niche.

Age- and region-dependent pattern of neurogenic and gliogenic activity in NSC cultures: effect of time in culture

Besides proliferation and long-term self-renewal, long-term multipotency remains the defining property of a bona fide NSC, and this property distinguishes this cell from transient amplifying progenitors. We verified multipotency in our bulk NSC lines at early and late subculturing passages, adding a third variable (time in culture) to the two previously considered (SVZ region and postnatal age). Interestingly, we documented that the age-dependent increase in astroglial/neuronal cell ratio mainly depends on a decrease in the number of neurons and resembles that observed in primary cultures (this study) and in the postnatal/adult SVZ neurogenic niche in vivo (Peretto et al.,2005).

In primary cultures, decreased numbers of neuronal progenitors retrieved from the original tissue might well explain our observations, although we cannot exclude a concomitant change in cell fate commitment, which might involve both neuronal and astroglial progenitors. Higher numbers of TUJ1+ with respect to MAP2+ cells likely reflect the enrichment in neuroblasts at the expense of mature neurons due to tissue harvesting and dissociation. In addition, their incomplete maturation may be due to limited differentiation time in culture.

We tend to exclude that decreased number of neurons in NSC-derived progeny might result from an overall decrease in NSC proliferation, given the moderate age-dependent decrease of NSC growth rates, at least in LV-derived NSC lines. Reduced proliferation capacity of committed neuronal progenitors and/or increased proliferation of glial progenitors might explain our results. Indeed, we have found that there are higher proportions of proliferating (Ki67+) glial cells (GFAP+/nestin+) compared to neuronal (TUJ1+) cells in NSC-derived differentiated cultures (A. Gritti, pers. obs.). Further, we cannot rule out changes in cell death among different cell types nor the shift in progenitor commitment toward the glial at the expense of the neuronal fate. Regardless of the potential mechanism/s accounting for the age-dependent reduction in neurogenic capacity, this was maintained in late-passage NSC cultures, suggesting that this effect may be ascribed to an intrinsic developmental program of primary precursors and/or their proliferative progeny. Further studies are needed to address these issues.

In turn, the decreased number of neurons generated from late- with respect to early-passage NSCs might suggest a process of in vitro “aging” of stem cells/progenitors (as a result of extensive culturing) that mimics that occurring in the neurogenic compartments in vivo. A similar effect was previously reported in murine embryonic (Smith et al.,2003; Pagani et al.,2006) and human fetal (Wright et al.,2006) neural stem/progenitor cultures. In our hands, this effect was more evident in neonatal and early postnatal- than in adult-derived NSC cultures. This is consistent with data showing that adult NSCs maintain stable functional features in long-term cultures (Foroni et al.,2007) and suggests that the neurogenic capacity of adult NSCs might be a type of functional endpoint that is achieved under the selective in vitro culture conditions imposed by the NSA. In support of this hypothesis, we found an analogy between the proportion of neurons generated by neonatal NSCs maintained long-term in vitro and the adult NSCs at early subculturing passages. For example, percentages of TUJ1+ cells in 10th-passage neonatal LV cultures (16.54% ± 1.19%; P0) are comparable to those found in 3rd passage adult NSCs (14.05% ± 1.36% and 10.30% ± 1.53%; P21 and P90, respectively).

The reduced percentages of TUJ1+ neurons in OB-derived primary cultures and in RE-derived NSC progeny with respect to their LV-derived counterparts, regardless the postnatal age considered or the time in culture, might be due to region-intrinsic differences in the precursor capacity to generate neuroblasts. Alternatively, OB/RE neuroblasts might display a higher commitment to differentiation/maturation with respect to their LV counterpart (Hack et al.,2005). The presence of similar numbers of MAP2-expressing neurons in LV and RE cultures together with data from the bulk population analysis seems to support this

hypothesis. Despite the quantitative differences, late-passage RE-derived neurons maintained a morphology resembling that observed in early-passaged NSC cultures and in primary OB cultures.

Despite the age-dependent reduction in number, the LV- and RE-derived neuronal populations maintained neurochemical heterogeneity, as shown by the presence of the main neuronal subtypes that we observed in OB-derived primary cultures and that are described in vivo (Parrish-Aungst et al.,2007; Bagley et al.,2007; Batista-Brito et al.,2008).

It is known that cells of the glial lineage undergo dramatic changes during the postnatal modification of the SVZ region (Peretto et al.,2005), as a consequence of both intrinsic developmental programs and of cell-extrinsic cues provided by the niche environment (Tropepe et al.,1997; Jin et al.,2003; Maslov et al.,2004). Although we did not perform a quantitative analysis, we observed region-dependent differences in astroglial and neuronal morphology that were independent from the age of donor tissue, likely representing region-dependent intrinsic features of glial and neuronal progenitors. Also, the morphological and antigenic heterogeneity of the glial cell population observed in our primary cultures resembled that which characterizes glial populations at the neurogenic sites. This was true also for the glial population in NSC-derived progeny, although in these cultures the typical morphology that distinguished OB from LV-derived astrocytes in primary cultures and in the progeny of early-passage RE-derived NSCs was lost.

Importantly, we observed an age-dependent decrease and regional differences in the number of oligodendroglial cells in both primary cultures and in NSC-derived cultures, indicating that either the size or the function of oligodendrocyte progenitor pool residing in these regions (Aguirre et al.,2004; Menn et al.,2006) are affected. The existence of a common neuronal/oligodendroglial progenitor (Hack et al.,2005) might also account for the similar age-dependent trend that we observe in these two cell types.

CONCLUSION

To our knowledge this study is the first in vitro systematic analysis performed on bona fide NSC populations (related to age- and region-matched primary cultures) in a comprehensive time course that accounts for three critical variables: developmental age, SVZ region, and time in culture, during the postnatal changes that ultimately define the features of the adult SVZ neurogenic niche (Tramontin et al.,2003; Peretto et al.,2005). We focused on the postnatal period in which the SVZ niche adapts from an embryonic germinal layer (building up the CNS) to an adult neurogenic site (sustaining adult neurogenesis within restricted brain regions), in order to evaluate whether intrinsic NSC properties, in addition to the occurrence of well-known changes in the anatomical and molecular environment of the niche, could explain the age-related changes in the neurogenic activity.

Emerging evidence suggests significant heterogeneity of primary precursors in the SVZ niche, which appear to possess an intrinsic and restricted neurogenic program (Merkle et al.,2007; Young et al.,2007) and the capability of producing oligodendrocytes in addition to olfactory interneurons (Menn et al.,2006; Cheng et al.,2009). While it is known that both cell-intrinsic and environmental factors contribute to restriction of stem cell and neuronal progenitor competency during cortical development (Shen et al.,2006), the mechanisms that restrict stem cell potential in the postnatal/adult neurogenic niches are largely unknown. Maintenance of specific gliogenic and, most interestingly, neurogenic capacity in primary cultures and serially passaged NSC cultures isolated from their niche, as described in our systematic analysis, further suggests an intrinsic competence of NSCs (considering either individual cells or populations of cells) regarding fate commitment and survival/differentiation of newborn progeny, as a function of postnatal brain development. Besides transcription factors, some of which are well known regulators of neurogenesis and NSC function (Merkle and Alvarez-Buylla,2006; Wang et al.,2006; Wen et al.,2008), the potential role of small, noncoding RNAs in exerting a tight posttranscriptional regulation of gene expression during nervous system development and in neural stem/progenitor cell activity is now being actively investigated (De Pietri Tonelli et al.,2008; Nishino et al.,2008; Zeng,2008; Cheng et al.,2009). Further studies will be required to comprehensively determine the intrinsic factors that contribute to this competence. These factors play a role in defining the capacity of NSC populations to appropriately respond to microenvironmental signals (Sheen et al.,1999), i.e., those dynamically present in the niche during postnatal development. Understanding this, ex vivo isolation and extensive in vitro culture under strong and defined mitogen selection would result in a mismatch between intrinsic NCS competence and microenvironment. This might explain the partial drift in the functional features that we and others observed in long-term cultured NSCs as well as the reported ability of serially passaged NSCs to integrate and differentiate properly if placed in a homolog environment (Herrera et al.,1999; Klein et al.,2005). Understanding the respective contribution provided by intrinsic and extrinsic cues on NSC behavior will pave the way to manipulation of NSC fate potential for therapeutic approaches aimed at repairing diseased or injured brain.

Acknowledgements

We thank Dr. A.L. Vescovi, since part of this work was performed in his laboratory at the Stem Cell Research Institute, San Raffaele Scientific Institute. We thank Sarah Haecker for critically revising the article.

LITERATURE CITED

- Aguirre AA, Chittajallu R, Belachew S, Gallo V. 2004. NG2-expressing cells in the subventricular zone are type C-like cells and contribute to interneuron generation in the postnatal hippocampus. J Cell Biol 165: 575–589.

- Alvarez-Buylla A, Seri B, Doetsch F. 2002. Identification of neural stem cells in the adult vertebrate brain. Brain Res Bull 57: 751–758.

- Alves JA, Barone P, Engelender S, Froes MM, Menezes JR. 2002. Initial stages of radial glia astrocytic transformation in the early postnatal anterior subventricular zone. J Neurobiol 52: 251–265.

- Bagley J, LaRocca G, Jimenez DA, Urban NN. 2007. Adult neurogenesis and specific replacement of interneuron subtypes in the mouse main olfactory bulb. BMC Neurosci 8: 92.

- Batista-Brito R, Close J, Machold R, Fishell G. 2008. The distinct temporal origins of olfactory bulb interneuron subtypes. J Neurosci 28: 3966–3975.

- Bonfanti L, Peretto P. 2006. Radial glial origin of the adult neural stem cells in the subventricular zone. Prog Neurobiol 83: 24–36.

- Bouilleret V, Loup F, Kiener T, Marescaux C, Fritschy JM. 2000. Early loss of interneurons and delayed subunit-specific changes in GABA(A)-receptor expression in a mouse model of mesial temporal lobe epilepsy. Hippocampus 10: 305–324.

- Cavazzin C, Ferrari D, Facchetti F, Russignan A, Vescovi AL, La Porta CA, Gritti A. 2006. Unique expression and localization of aquaporin-4 and aquaporin-9 in murine and human neural stem cells and in their glial progeny. Glia 53: 167–181.

- Chalazonitis A, Pham TD, Li Z, Roman D, Guha U, Gomes W, Kan L, Kessler JA, Gershon MD. 2008. Bone morphogenetic protein regulation of enteric neuronal phenotypic diversity: relationship to timing of cell cycle exit. J Comp Neurol 509: 474–492.

- Cheng LC, Pastrana E, Tavazoie M, Doetsch F. 2009. miR-124 regulates adult neurogenesis in the subventricular zone stem cell niche. Nat Neurosci 12: 399–408.

- Consiglio A, Gritti A, Dolcetta D, Follenzi A, Bordignon C, Gage FH, Vescovi AL, Naldini L. 2004. Robust in vivo gene transfer into adult mammalian neural stem cells by lentiviral vectors. Proc Natl Acad Sci U S A 101: 14835–14840.

- Conti L, Pollard SM, Gorba T, Reitano E, Toselli M, Biella G, Sun Y, Sanzone S, Ying QL, Cattaneo E, Smith A. 2005. Niche-independent symmetrical self-renewal of a mammalian tissue stem cell. PLoS Biol 3: e283.

- Copray S, Balasubramaniyan V, Lavenga J, de Bruijn J, Liem R, Boddeke E. 2006. Olig2 overexpression induces the in vitro differentiation of neural stem cells into mature oligodendrocytes. Stem Cells 24: 1001–1010.

- De Pietri Tonelli D, Pulvers JN, Haffner C, Murchison EP, Hannon GJ, Huttner WB. 2008. miRNAs are essential for survival and differentiation of newborn neurons but not for expansion of neural progenitors during early neurogenesis in the mouse embryonic neocortex. Development 135: 3911–3921.

- Doetsch F. 2003. A niche for adult neural stem cells. Curr Opin Genet Dev 13: 543–550.

- Doetsch F, Caille I, Lim DA, Garcia-Verdugo JM, Alvarez-Buylla A. 1999. Subventricular zone astrocytes are neural stem cells in the adult mammalian brain. Cell 97: 703–716.

- Doetsch F, Petreanu L, Caille I, Garcia-Verdugo JM, Alvarez-Buylla A. 2002. EGF converts transit-amplifying neurogenic precursors in the adult brain into multipotent stem cells. Neuron 36: 1021–1034.

- Ferrari D, Sanchez-Pernaute R, Lee H, Studer L, Isacson O. 2006. Transplanted dopamine neurons derived from primate ES cells preferentially innervate DARPP-32 striatal progenitors within the graft. Eur J Neurosci 24: 1885–1896.

- Foroni C, Galli R, Cipelletti B, Caumo A, Alberti S, Fiocco R, Vescovi A. 2007. Resilience to transformation and inherent genetic and functional stability of adult neural stem cells ex vivo. Cancer Res 67: 3725–3733.

- Furmanski O, Gajavelli S, Lee JW, Collado ME, Jergova S, Sagen J. 2009. Combined extrinsic and intrinsic manipulations exert complementary neuronal enrichment in embryonic rat neural precursor cultures: an in vitro and in vivo analysis. J Comp Neurol 515: 56–71.

- Gage FH. 2000. Mammalian neural stem cells. Science 287: 1433–1438.

- Gritti A, Parati EA, Cova L, Frolichsthal P, Galli R, Wanke E, Faravelli L, Morassutti DJ, Roisen F, Nickel DD, Vescovi AL. 1996. Multipotential stem cells from the adult mouse brain proliferate and self-renew in response to basic fibroblast growth factor. J Neurosci 16: 1091–1100.

- Gritti A, Frolichsthal-Schoeller P, Galli R, Parati EA, Cova L, Pagano SF, Bjornson CR, Vescovi AL. 1999. Epidermal and fibroblast growth factors behave as mitogenic regulators for a single multipotent stem cell-like population from the subventricular region of the adult mouse forebrain. J Neurosci 19: 3287–3297.

- Gritti A, Bonfanti L, Doetsch F, Caille I, Alvarez-Buylla A, Lim DA, Galli R, Verdugo JM, Herrera DG, Vescovi AL. 2002. Multipotent neural stem cells reside into the rostral extension and olfactory bulb of adult rodents. J Neurosci 22: 437–445.

- Hack MA, Saghatelyan A, de Chevigny A, Pfeifer A, Ashery-Padan R, Lledo PM, Gotz M. 2005. Neuronal fate determinants of adult olfactory bulb neurogenesis. Nat Neurosci 8: 865–872.

- Haubensak W, Attardo A, Denk W, Huttner WB. 2004. Neurons arise in the basal neuroepithelium of the early mammalian telencephalon: a major site of neurogenesis. Proc Natl Acad Sci U S A 101: 3196–3201.

- Herrera DG, Garcia-Verdugo JM, Alvarez-Buylla A. 1999. Adult-derived neural precursors transplanted into multiple regions in the adult brain. Ann Neurol 46: 867–877.

- Hockfield S, McKay RD. 1985. Identification of major cell classes in the developing mammalian nervous system. J Neurosci 5: 3310–3328.

- Iglesia DD, Gala PH, Qiu T, Stepp MA. 2000. Integrin expression during epithelial migration and restratification in the tenascin-C-deficient mouse cornea. J Histochem Cytochem 48: 363–376.

- Irvin DK, Dhaka A, Hicks C, Weinmaster G, Kornblum HI. 2003. Extrinsic and intrinsic factors governing cell fate in cortical progenitor cultures. Dev Neurosci 25: 162–172.

- Jin K, Sun Y, Xie L, Batteur S, Mao XO, Smelick C, Logvinova A, Greenberg DA. 2003. Neurogenesis and aging: FGF-2 and HB-EGF restore neurogenesis in hippocampus and subventricular zone of aged mice. Aging Cell 2: 175–183.

- Klein C, Butt SJ, Machold RP, Johnson JE, Fishell G. 2005. Cerebellum- and forebrain-derived stem cells possess intrinsic regional character. Development 132: 4497–4508.

- Kohwi M, Petryniak MA, Long JE, Ekker M, Obata K, Yanagawa Y, Rubenstein JL, Alvarez-Buylla A. 2007. A subpopulation of olfactory bulb GABAergic interneurons is derived from Emx1- and Dlx5/6-expressing progenitors. J Neurosci 27: 6878–6891.

- Lemasson M, Saghatelyan A, Olivo-Marin JC, Lledo PM. 2005. Neonatal and adult neurogenesis provide two distinct populations of newborn neurons to the mouse olfactory bulb. J Neurosci 25: 6816–6825.

- Lledo PM, Alonso M, Grubb MS. 2006. Adult neurogenesis and functional plasticity in neuronal circuits. Nat Rev Neurosci 7: 179–193.

- Lois C, Alvarez-Buylla A. 1994. Long-distance neuronal migration in the adult mammalian brain. Science 264: 1145–1148.

- Luo J, Daniels SB, Lennington JB, Notti RQ, Conover JC. 2006. The aging neurogenic subventricular zone. Aging Cell 5: 139–152.

- Manzke T, Preusse S, Hulsmann S, Richter DW. 2008. Developmental changes of serotonin 4(a) receptor expression in the rat pre-Botzinger complex. J Comp Neurol 506: 775–790.

- Maslov AY, Barone TA, Plunkett RJ, Pruitt SC. 2004. Neural stem cell detection, characterization, and age-related changes in the subventricular zone of mice. J Neurosci 24: 1726–1733.

- Menn B, Garcia-Verdugo JM, Yaschine C, Gonzalez-Perez O, Rowitch D, Alvarez-Buylla A. 2006. Origin of oligodendrocytes in the subventricular zone of the adult brain. J Neurosci 26: 7907–7918.

- Merkle FT, Alvarez-Buylla A. 2006. Neural stem cells in mammalian development. Curr Opin Cell Biol 18: 704–709.

- Merkle FT, Tramontin AD, Garcia-Verdugo JM, Alvarez-Buylla A. 2004. Radial glia give rise to adult neural stem cells in the subventricular zone. Proc Natl Acad Sci U S A 101: 17528–17532.

- Merkle FT, Mirzadeh Z, Alvarez-Buylla A. 2007. Mosaic organization of neural stem cells in the adult brain. Science 317: 381–384.

- Nishino J, Kim I, Chada K, Morrison SJ. 2008. Hmga2 promotes neural stem cell self-renewal in young but not old mice by reducing p16Ink4a and p19Arf Expression. Cell 135: 227–239.

- Pagani F, Lauro C, Fucile S, Catalano M, Limatola C, Eusebi F, Grassi F. 2006. Functional properties of neurons derived from fetal mouse neurospheres are compatible with those of neuronal precursors in vivo. J Neurosci Res 83: 1494–1501.

- Parrish-Aungst S, Shipley MT, Erdelyi F, Szabo G, Puche AC. 2007. Quantitative analysis of neuronal diversity in the mouse olfactory bulb. J Comp Neurol 501: 825–836.

- Pastrana E, Cheng LC, Doetsch F. 2009. Simultaneous prospective purification of adult subventricular zone neural stem cells and their progeny. Proc Natl Acad Sci U S A 106: 6387–6392.

- Peretto P, Giachino C, Aimar P, Fasolo A, Bonfanti L. 2005. Chain formation and glial tube assembly in the shift from neonatal to adult subventricular zone of the rodent forebrain. J Comp Neurol 487: 407–427.

- Ray J, Gage FH. 2006. Differential properties of adult rat and mouse brain-derived neural stem/progenitor cells. Mol Cell Neurosci 31: 560–573.

- Reynolds BA, Rietze RL. 2005. Neural stem cells and neurospheres—re-evaluating the relationship. Nat Methods 2: 333–336.

- Reynolds BA, Weiss S. 1992. Generation of neurons and astrocytes from isolated cells of the adult mammalian central nervous system. Science 255: 1707–1710.

- Sanchez-Pernaute R, Studer L, Ferrari D, Perrier A, Lee H, Vinuela A, Isacson O. 2005. Long-term survival of dopamine neurons derived from parthenogenetic primate embryonic stem cells (cyno-1) after transplantation. Stem Cells 23: 914–922.

- Seaberg RM, van der Kooy D. 2002. Adult rodent neurogenic regions: the ventricular subependyma contains neural stem cells, but the dentate gyrus contains restricted progenitors. J Neurosci 22: 1784–1793.

- Seaberg RM, van der Kooy D. 2003. Stem and progenitor cells: the premature desertion of rigorous definitions. Trends Neurosci 26: 125–131.

- Seaberg RM, Smukler SR, van der Kooy D. 2005. Intrinsic differences distinguish transiently neurogenic progenitors from neural stem cells in the early postnatal brain. Dev Biol 278: 71–85.

- Sheen VL, Arnold MW, Wang Y, Macklis JD. 1999. Neural precursor differentiation following transplantation into neocortex is dependent on intrinsic developmental state and receptor competence. Exp Neurol 158: 47–62.

- Shen Q, Wang Y, Dimos JT, Fasano CA, Phoenix TN, Lemischka IR, Ivanova NB, Stifani S, Morrisey EE, Temple S. 2006. The timing of cortical neurogenesis is encoded within lineages of individual progenitor cells. Nat Neurosci 9: 743–751.

- Smith R, Bagga V, Fricker-Gates RA. 2003. Embryonic neural progenitor cells: the effects of species, region, and culture conditions on long-term proliferation and neuronal differentiation. J Hematother Stem Cell Res 12: 713–725.

- Tramontin AD, Garcia-Verdugo JM, Lim DA, Alvarez-Buylla A. 2003. Postnatal development of radial glia and the ventricular zone (VZ): a continuum of the neural stem cell compartment. Cereb Cortex 13: 580–587.

- Tropepe V, Craig CG, Morshead CM, van der Kooy D. 1997. Transforming growth factor-alpha null and senescent mice show decreased neural progenitor cell proliferation in the forebrain subependyma. J Neurosci 17: 7850–7859.

- Wang TW, Stromberg GP, Whitney JT, Brower NW, Klymkowsky MW, Parent JM. 2006. Sox3 expression identifies neural progenitors in persistent neonatal and adult mouse forebrain germinative zones. J Comp Neurol 497: 88–100.

- Wen S, Li H, Liu J. 2008. Epigenetic background of neuronal fate determination. Prog Neurobiol 87: 98–117.

- Wright LS, Prowse KR, Wallace K, Linskens MH, Svendsen CN. 2006. Human progenitor cells isolated from the developing cortex undergo decreased neurogenesis and eventual senescence following expansion in vitro. Exp Cell Res 312: 2107–2120.

- Young KM, Fogarty M, Kessaris N, Richardson WD. 2007. Subventricular zone stem cells are heterogeneous with respect to their embryonic origins and neurogenic fates in the adult olfactory bulb. J Neurosci 27: 8286–8296.

- Zeng Y. 2008. Regulation of the mammalian nervous system by microRNAs. Mol Pharmacol 75: 259–264.